Numerical Validation of the Power Performance of HAWT (Ge 1.5xle) by Computational Fluid Dynamic of the Manufacturing Technical Data

Mohamed Higaeg
Mechanical Engineering Department, Misurata Technical Science Collage
Misurata.Libya

Abdullah Alajail
Petroleam Engineering Department, Faculty of Engineering, Misurata University
Misurata.Libya

Abstract-- **This paper was conducted to characterize the aerodynamic behaviour of the blade wind turbine (Ge1.5xle) by computational fluid dynamics (CFD), the simulation was performed typical to the blade of Ge1.5xle which is 41.25 m length using three different airfoils S818, S825 and S826 for the blade root, primary and tip respectively. The blade was added one meter for fixation to the hub of rotation. The blade designed to be twist by 42 degrees from first airfoil place to the last one at the tip of the blade with attack angle is 4 degree based on the specification of the wind turbine Ge 1.5xle to enable comparison the results of computational fluid dynamics (CFD) with the specification data of wind turbine mentioned above, also with the theoretical calculations. The results of simulation at rated wind speed 11.5 (m/s) are agreed with the specification data of the wind turbine such as the aerodynamic efficiency is 29 (%), but obvious variation is observed for blade tip speed. Furthermore, the velocity vectors are in good agreement with flow characteristic and the flow was perfectly attached and there is no flow separation over the three different airfoils used.**

I. INTRODUCTION

Recently, the world demand has increased of the energy through a rise of human life level. The results of the oil price raise and its environment influence, the scientific researchers have been performed on the renewable energy as the alternatives of fossil fuels which are the wind energy one of renewable energy applications and it is the most promising sources of the renewable energy.

The wind energy can be converted into mechanical power through blades which are the most vital component of wind turbine. Blades play a major part in wind turbines and they have more potential of the wind turbine efficiency/performance improvement to capture a more energy from wind. The efficiency of wind turbine blades depends on the number of factors (such as the blade shape and material) where the blade shape controls the aerodynamic characteristics and the pressure distribution in service. The most important parameters of the blade material are to be high stiffness, low density and long hypothetical life. Nowadays, the composite materials have been used for a fabrication of the wind turbine blades to reduce the blade weight in turn decreasing the gravity effect load.

The numerical investigation of power coefficient of horizontal axis 3-blades wind turbine implemented and compared with experimental data for the same tip speed ratio, and the results were a good agreement with an estimation error of about 5% [1]. The performance analysis of a small horizontal axis wind turbine predicted at low Reynolds number using blade element momentum theory and using Computational Fluid Dynamics (CFD) and experiment. The performance was analysed for wind speeds between 2m/s to 7m/s. Studies showed that the blade is capable of generating power up to 241W with a power coefficient of 34.3% at a speed of 6m/s. The computed power coefficient is in a good agreement with experimental results 33.7% [2].

The main goal of this paper is to analyze the flow field around the blade of horizontal axis Ge1.5xle wind turbine by numerical solving the governing equations of Continuity [3] and Momentum Equations and the Reynolds-averaged Navier-Stokes (RANS) equations [4]. Upstream and downstream wake visualization in three dimensions velocities are scope of the paper. Furthermore, the tangential velocity at the tip of blade and the wind turbine dynamic performance will be plotted and compared with the theoretical and technical data of horizontal axis Ge1.5xle wind turbine.

II. BLADY GEOMETRY

A. Blade Airfoil Selection

The rotor blade designs in 41.25 m length category, hence three different airfoils were selected and distributed along the blade. The airfoils distribute in the blade root, primary and tip regions. The proposal of airfoils at the root of the blade is mainly structural, contributing to the aerodynamics performance of the blade but at a lower level. Thus, the root of the blade is bigger and stronger than the other two airfoils used at the primary and tip regions. The airfoils closer to the tip of the blade generate higher lift due to speed variation in the relative wind [5]. Firstly, we started by selection of airfoils. We chose to use the NREL S-series of airfoil as described in

(Malcom and Hansen). These airfoils are in general somewhat thicker than the types typically seen on airplanes due to structural concerns, and are largely insensitive to roughness. The set of three airfoils are defining a single blade with a variable cross section, such that the blade root airfoil (S818) is the cross-section shape at the location of largest chord length, the blade primary airfoil (S825) is the shape at 75% of the blade radius, and the blade tip airfoil (S826) which occurs at 95% of the radius. The airfoils data are gathered from the NREL documents and are validated to be accurate with XFLR, and figure (1), shows the blade airfoils profile of NREL S818, S825, and S826 respectively [6].
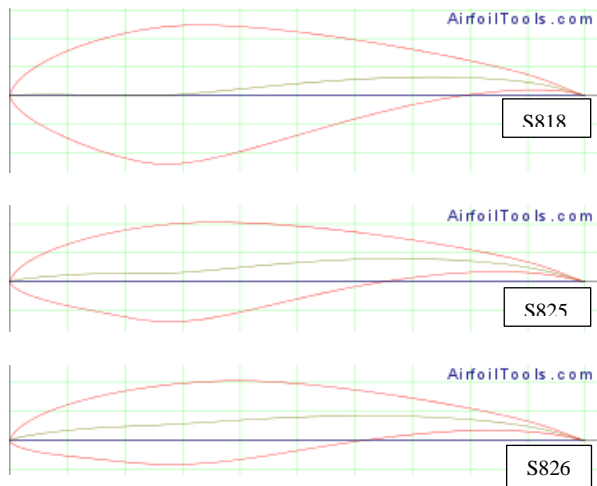

Figure (1). Airfoils Profile of NREL (S818, S825, S826)

B. Blade Geometry

The determination of the blade shape depends on the airfoils selection in the whole blade, which were designed for wind turbine blade by CATIA V5R20 software. The Blade is 41.25 m long, it was divided into a twenty elements starting from blade root, and it was twisted 42 degrees from root section to tip. The shape distribution of the blade starts by circular hub section. This circular shape transfers into own profile, then it transits to S818 in the root region, and it converts to airfoil S825 in blade primary region, and then converting to airfoil S826 at the blade tip region in sequence as shown in table (1).

Table (1) Wind Turbine Blade Geometry

element	r/R	Twist (Deg)	Chord (m)	Airfoil
1	0.075	42	2.5328	
2	0.125	32	2.8157	
3	0.175	23	3.0740	
4	0.225	15	3.2101	
5	0.275	11.5	3.1115	S818
6	0.325	8.2	2.9651	
7	0.375	7	2.8182	
8	0.425	6	2.6726	
9	0.475	5	2.5270	
10	0.525	4	2.3805	
11	0.575	4.15	2.2337	
12	0.625	3.85	2.0881	
13	0.675	3.25	1.9416	S825
14	0.725	2.75	1.7985	
15	0.775	1.25	1.6599	
16	0.825	0.75	1.5279	
17	0.875	0.55	1.3963	
18	0.925	0.85	1.2647	S826
19	0.975	0.05	1.1331	
20	1	0	1.0000	

After the design of the blade geometry was completed, then the blade geometry is imported into computational fluid dynamics (CFD) analysis systems, That's important for the prediction of the blade aerodynamic performance at variation of wind conditions in order to obtain the distribution of pressure loads on the blade surface to use it in Static and transient Structural Analysis Systems.

III.   NUMERICAL MODELLING

Mathematical models and algorithms are required to perform numerical analysis of fluid -structure interaction. Computational fluid dynamics (CFD) is a section of the fluid mechanics which is used for numerical modelling and simulation of fluid flows. Finite element analysis is used for analysis of the structural behaviour under various boundary conditions.

A.   Continuity and Momentum Equations

The evolution of a fluid element is governed by two conservation laws: the conservation of mass and the conservation of momentum. Mass conservation leads to the continuity equation and can be written as follows [3]:

$$\frac{\partial \rho}{\partial t} + \nabla \cdot (\rho \vec{u}) = 0 \qquad (1)$$

The equation above is the general form of mass conservation equation and is valid for incompressible as well as compressible flows.

Conservation of momentum in an inertial (non-accelerating) reference frame can be described [7]:

$$\frac{\partial}{\partial t}(\rho \vec{u}) + \nabla \cdot (\rho \vec{u}\vec{u}) = -\nabla p + \nabla \cdot (\overline{\overline{\tau}}) + \rho \vec{g} + \vec{F} \qquad (2)$$

Where p is the static pressure, $\overline{\overline{\tau}}$ is the stress tensor (described below), and $\rho\vec{g}$ and $\vec{F}$ are the gravitational body force and external body forces respectively. $\vec{F}$ also contains other model-dependent source terms such as porous-media and user-defined sources.

The stress tensor $\overline{\overline{\tau}}$ is given by:

$$\overline{\overline{\tau}} = \mu[(\nabla\vec{u} + \nabla\vec{u}^T) - \frac{2}{3}\nabla \cdot \vec{u}I] \qquad (3)$$

Where μ is the molecular viscosity, I is the unit tensor, and second term on the right hand side is the effect of volume dilation.

B.   Reynolds Averaged Navier Stokes (RANS) Equations

The Reynolds-averaged Navier-Stokes (RANS) equations are related to the fluid flow motion of the time-averaged. These equations are utilized firstly during the application of the turbulent flow. These equations with approximation are utilized to obtain approximate average solutions to the Navier-Stokes equations depending on the knowledge of turbulence flow properties. The equations can be written in Cartesian tensor form as [4]:

$$\frac{\partial \rho}{\partial t} + \frac{\partial}{\partial x_i}(\rho u_i) = 0 \qquad (4)$$

$$\frac{\partial}{\partial t}(\rho u_i) + \frac{\partial}{\partial x_j}(\rho u_i u_j)$$
$$= -\frac{\partial p}{\partial x_i} + \frac{\partial}{\partial x_j}\left[\mu(\frac{\partial u_i}{\partial x_j} + \frac{\partial u_j}{\partial x_i} - \frac{2}{3}\delta_{ij}\frac{\partial u_I}{\partial x_I}\right]$$
$$+ \frac{\partial}{\partial x_j}(-\rho\overline{u_i'u_j'}) \qquad (5)$$

These two equations (4) and (5) are called Reynolds-averaged Navier-Stokes (RANS) equations. In the instantaneous of solution variables in both Reynolds averaging and Navier-Stokes equations are analysed into ensemble-averaged/time averaged and fluctuating components such as the velocity components:

$$u_i = \overline{u_i} + u_i' \qquad (6)$$

Where $\overline{u_i}$ and u_i' are the mean and fluctuating velocity components (i=1,2,3).

Also the same, for pressure and other scalar quantities:

$$\varphi = \overline{\varphi} + \varphi' \qquad (7)$$

Where φ symbolizes a scalar such as pressure, energy, or species concentration.

C. Turbulence Models

The velocity fluctuation inducts the flow to be turbulent; these fluctuations generate a mixture of the transported quantities as momentum, energy, and species concentration, and also fluctuate the transported quantities. Since these fluctuations can be in the small scale form and high frequency, the simulation of this form is more computationally expensive. The instantaneous equations of continuity and momentum are accounted to be a time average, ensemble-averaged. These equations have additional contained flow unknown variables and turbulence models are applied to define these variables in turns known quantities [8]. The turbulent flow is defined by the Reynolds number.

The laminar flow can be considered when the Re number less than 1200, likewise the flow can be turbulent when the Re number is higher than that. The turbulent flow is described the fluid motion in a winding path. In this study, the design stream velocity is 8 m/s and based on the design velocity can be calculated Reynolds number which is ....., according to Reynolds number calculated, the flow is completely turbulent. Hence, the study assumption for the flow is to be incompressible flow.

There are different turbulence models in ANSYS fluent (CFD) can be chosen, such as:

· Spalart-Allmaras model
· k-ε models (standard, renormalization-group(RNG), realizable)
· k-ω models (standard, sheer-stress transport (SST))
· Transition SST models
· Reynolds Stress models (RSM)
· Detached eddy simulation (DES) model
· Large eddy simulation (LES) model

In this study, the turbulence model was chosen the shear stress transport k-ω model. The applications of a low of Reynolds number can use the k-ω SST model without extra damping functions. In the free stream, the SST formulation converts to a k-ε behaviour to avoid that the k-ω problem that

the model is very sensitive to the inlet stream turbulence properties. The turbulence model k-ω SST computes for its good behaviour in adverse pressure gradients and flow separation [9].

IV. THEORETICAL CALCULATIONS

A. Blade Tip Speed

According to the specification sheet of the GE 1.5xle wind turbine, theoretically can be calculated the Blade tip speed. We can then later compare this result with what we get from our simulation to verify that they agree. The blade tip speed (V) can obtain by apply the following formula:

$$V = r.\omega \qquad (8)$$

Plugging in our angular velocity of 2.22 rad/s and using the blade length of 41.2 meters plus one meter to account for the distance from the root to the hub, we get 42.25 meters. Therefore the tip speed is:

$$V = 2.22 * 42.25 = 93.8 \text{ (m/s)}$$

Additionally, by using the simple one-dimensional momentum theory, we can estimate the power coefficient which is the fraction of harnessed power to total power in the wind for the given turbine swept area. This analysis uses the following assumptions:

a. The flow is steady, homogenous and incompressible.
b. There is no frictional drag.
c. There is an infinite number of blades.
d. There is uniform thrust over the disc or rotor area.
e. The wake is non-rotating.
f. The static pressure far upstream and downstream of the rotor is equal to the undisturbed   ambient pressure.

B. Power Coefficient

The designed blade supposed to resemble GE 1.5xle wind turbine blade [10]. Referring to the wind turbine Ge1.5xle specification sheet demonstrates rated power 1.5 MW at rated wind velocity 11.5 m/s for rotor diameter to be 84.5 m. A power coefficient [11] is then defined as:

$$P = T.\omega \qquad (9)$$

$$C_P = \frac{P_{rated}}{P_{wind}} = \frac{P_{rated}}{0.5\,\rho\,A\,V_{rated}^3} \qquad (10)$$

The resulting power coefficient of 28.7% it is very reasonable. We will compare it to power coefficient obtained from the simulation in the Verification and Conclusion section.

V. POWER COEFFICIENT

The power generated by the kinetic energy of a free flowing wind stream is shown in Figure (2), where is defined as the ratio of the power extracted by the wind turbine relative to the energy available in the wind stream. Power coefficient (C_p), represented as extracted power over the total power, it can be expressed by the induction factor (a) as:

$$C_p = 4a(1-a)^2 \qquad (11)$$

Where (a) is Induction factor, the fractional decrease in wind velocity between the free stream and rotor plane can be expressed in terms of an axial induction factor, a:

$$a = \frac{v_0 - v}{v_0} \qquad (12)$$

Where, v is the velocity at the disk and it is defined by:

$$v = \frac{1}{2}(v_0 + v_3) \qquad (13)$$

v_0 and v_3 are free stream and downstream velocities respectively. The amount of axial induction factor determines the amount of power extracted by turbine [6].
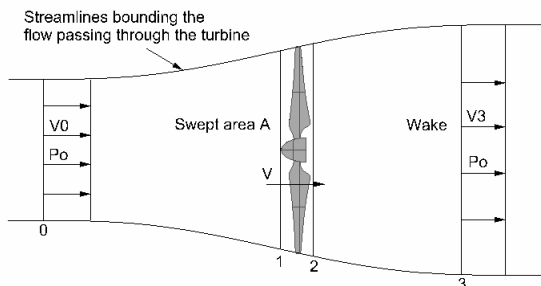

Figure (2). Control Volume for Idealized Actuator-disk Analysis

VI. BOUNDARY CONDITIONS

A. Computational Domain

The 3-D model of wind turbine contains three blades used which is symmetric, thus one blade was selected for numerical simulation has a length 41.25 (m) as shown in the figure (3). Rotational blade speed is defined at 21.2 (RPM). The flow around the blade is turbulent flow.
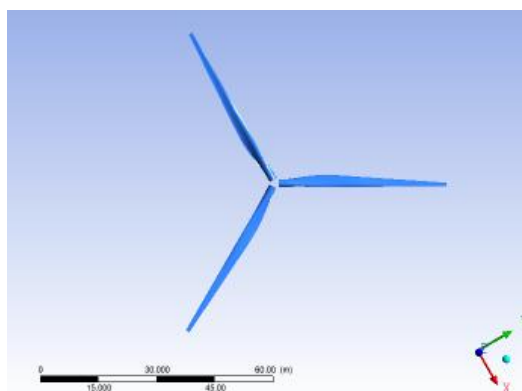

Figure (3). the Three Blades Wind Turbine Model

In this study for computation aerodynamic load on wind turbine blade was analyzed taking into respect an isolated blade with periodic boundaries, in order to make simulation a full three-blade rotor as much as a smaller domain, saving simulation time. For that, the 3-D domain is modelled as a semi-cylindrical section (conical shape) with a central angle of 120°. The domain inlet is planed 90 (m) ahead of the blade and the domain outlet 180 (m) behind the blade, and expands radially from the turbine axis of rotation to shroud at the 120 (m) radius in the inlet, and 240 (m) at the outlet, as

shown in the figure (4). The mode Boolean operation is applied for removal solid blade from the fluid domain; hence it creates a void in place of the blade. This void in the fluid domain is appropriate to implement CFD simulation.
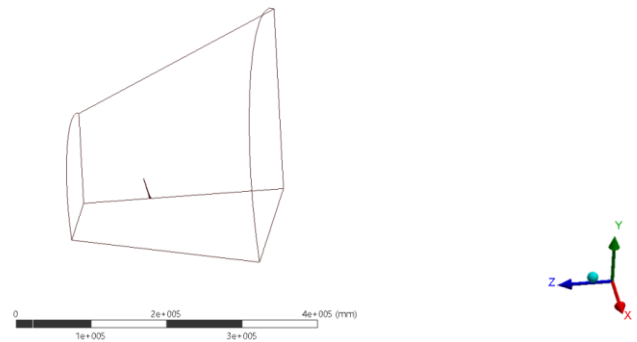

Figure (4). Fluent Domain of CFD

B. Numerical Mesh for CFD Computation

A number of local mesh controls have been applied to the numerical mesh for CFD computation to define the mesh feature in specific areas. The first model applied was the match control for matching the nodes for different surfaces. The second mode applied was inflation to specify cell size on the blade surface and captured the boundary layers on the object. The elements number of the mesh is 351988 which considered to be a very fine mesh quality. The mesh parameters help the CFD solver to converge with reducing the iterations and less error, that's can be obtained by keeping the quality of orthogonal ratio higher and skewness lower for whole CFD domain [12], where the quality average of orthogonal and skewness were 0.8364, 0.25617 respectively. Figure (5) shows the fluid domain mesh implementation. Through the observation, the mesh transition is a smooth, and a very accurate and small near to contact surfaces. The mesh control applications have been performed for obtaining the appropriate solutions.

The inlet velocity of boundary conditions can be set to the wind velocity free stream. The outlet pressure of the boundary condition assigns at atmospheric pressure. The domain outer surface can assign by the same of main inlet velocity. the fluent domain selected to be a conical shape based on the results experimental which have described that wake expansion behind the blade is formed conically [13,14]. The blade is chosen as the stationary non-slip wall, and the computational domain is taken into consideration to be a rotation frame by specified the rotational speed. The periodic boundary condition is applied for the computational domain reduced the number of grids to enable finer grids as shown in the figure (5) one-third of the turbine.

The air density and viscosity are chosen to be 1.225 kg/m³, 1.7894E-05 (kg/m.s) respectively, and the inlet turbulent intensity is 5%. In this study, the turbulence model is selected to be the k-ω shear stress transport (SST) model in the fluid solver: because it absorbs both the property of good accuracy in the near-wall region of standard k-ω model and nice precision in the far field region of k-ε model, it is more accurate and reliable for a wider class flow than the standard k-ω model. The most important features of the two-equation model developed by Menter [15] has the ability to transform from a k-ε

turbulence model [16] appropriate of the simulation far-field flows to a k-ω turbulence model [17] appropriate to modelling the boundary layer.
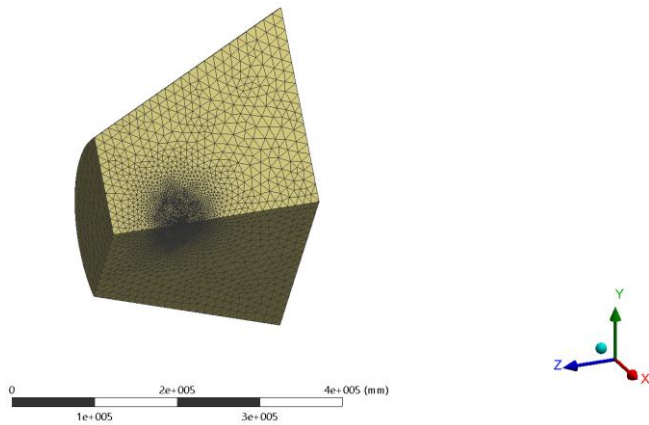

Figure (5). The Fluent Mesh

VII. Results and Discussion

At rated wind speed 11.5 (m/s), the velocity vector at three cross-sections selected which are defined as the blade radius percentage are in good agreement of flow characteristic and the flow is perfectly attached and there is no flow separation. We can be an obvious observation from figure (6) that the velocity vector on the upper surface is faster than the lower surface at the three different airfoils. Such as, for the blade tip region (0.92×R) the velocity vector is 112.2 (m/s) on the upper surface while the velocity vector on bottom surface approximately is 70 (m/s). The increase in velocity vector on upper surface creates a lower pressure and decrease in velocity vector on lower surface creates high pressure, this result of pressure difference creates lift force and it is higher in tip blade region compared with root and primary region.

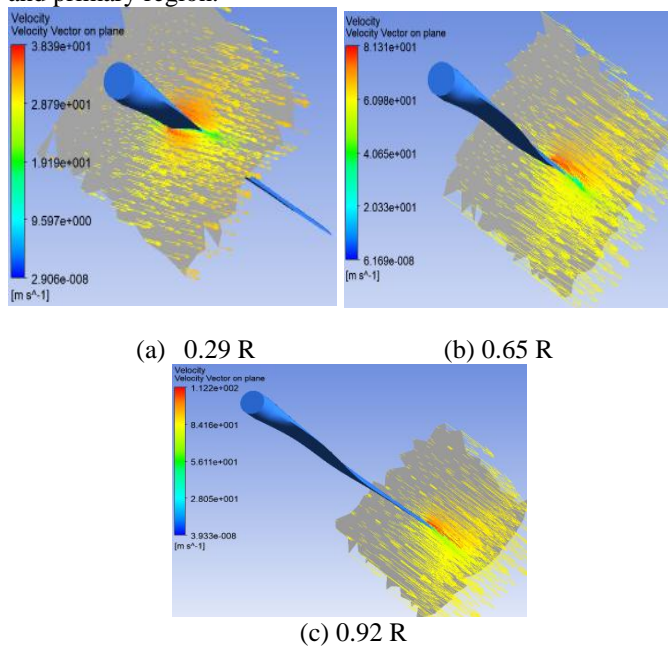(a)   0.29 R   (b) 0.65 R

(c) 0.92 R

Figure (6) Velocity Vector over Three Different Airfoils

In computational fluid dynamic (CFD)-post for the numerical results. We will enable the visualization of a full 3-blade wind turbine as shown in figure (7). The blade velocity obtained by the numerical analysis increases with increasing of rotor radius because it is the rotation of the blades. The tip blade velocity,

which is the highest velocity and it is equal 98.01 (m/s), while, the blade tip velocity obtained by theoretical calculation based on aerodynamic theory is 93.8 (m/s).
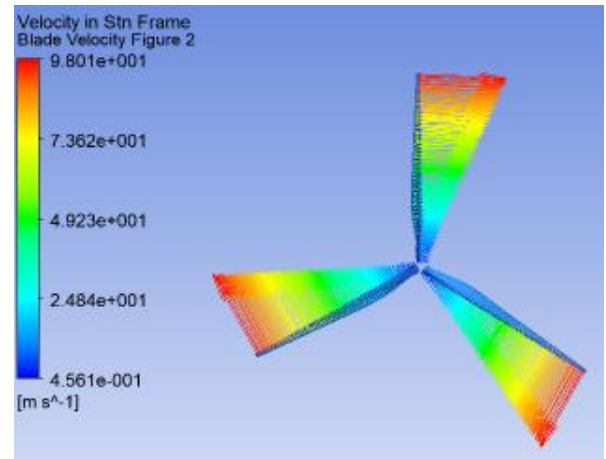

Figure (7). Blade Velocity

The fluid domain shows the wind velocity streamlines around the wind turbine blades as it illustrates in the figure (8). This figure record that, the wind velocity streamline is presented on colour graduation from blue to red explaining the change in the wind velocity streamline when it passes the blades of wind turbine. Wind turbine rotor extracts kinetic energy from wind, for that the wind velocity is decreased back of wind turbine as it shows in the figure (8), therefore it can be observation of velocity change from upstream wind which is the rated wind velocity and equal V_0=11.5 (m/s) and it is represented by green colour to downstream velocity and it is equal V_3=9.5 (m/s) and it is represented by blue colour.
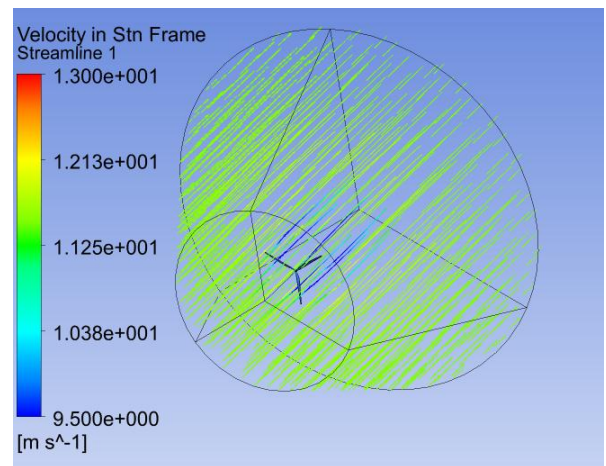

Figure (8). Velocity Streamlines

The wind turbine efficiency can be calculated according to the velocity streamlines values were obtained from fluent simulation which are the up-stream and down-stream velocities shown in the figure (8) and then applying these values on equations (6) to (8) to compute the wind turbine efficiency, and that equal C_p=29 %.

Table (2) demonstrates comparison results of tip blade velocity and the wind turbine efficiency for specification data, theoretical calculation and the Computational Fluid Dynamic (CFD) simulation results of The Ge 1.5 xle wind turbine

Table (2) Comparison Results

Parameter	Specification Data Sheet	Theoretical Calculation	CFD Results
Tip Blade Speed (m/s)	81 [18]	93.8	98.01
Power Coefficient C_p (%)	28.7	59	29

VIII. CONCLUSION

In present study, the performance of horizontal axis wind turbine is computed by implementation of the computational fluid dynamic (CFD), and these results are compared with the specification data of the Ge1.5xle wind turbine, also with the theoretical calculation. The computational fluid dynamics (CFD) result of the power coefficient is in agreement with the specification data of Ge1.5xle wind turbine has been published for the aerodynamic efficiency and this is the present study points, but obvious variation of blade tip velocity compared with the specification data. The velocity vectors at rated wind speed are observed around the three different airfoils using for the Ge1.5xle wind turbine show that, the flow characteristic is in good agreement and it is perfectly attached and it has not observe any flow separation. The velocity flow through the upper surface is faster than the lower surface for the three sections selected which causes the pressure difference and as result it creates the lift force. The velocity vector can be observed in higher velocity on upper blade surface than bottom surface, such as the velocity vectors at the blade section $(0.92 \times R)$ are 112.2 (m/s) for the upper surface and 70 (m/s) for the bottom surface. Finally, according to the results are obtained from the computational Fluid dynamics, this computational method can be applying for optimization of wind turbines.

REFERENCES

[1] Mohamed Ould Moussa. "*Experimental and Numerical Performances analysis of small Three* Blades Wind Turbine", Energy, vol.203, pp. 117807, 2020.

[2] Osarbo Ighodaro, David Akhihiero. "Modeling and Performance Analysis of a Small Horizontal Axis Wind Turbine", Journal of Energy Resources Technology, DOI: 10.1115/1.4047972, 2020.

[3] J. Jucha. "*Time-Symmetry Breaking in Turbulent Multi-Particle Dispersion*", Springer International Publishing Switzerland (2015), Springer Theses, DOI 10.1007/978-3-319-19192-8_2

[4] J. O. Hinze. "Turbulence", McGraw-Hill Publishing Co., New York. 1975.

[5] Naishadh G. Vasjaliya, Sathya N. Gangadharan, "Aero-Structural Design Optimization of Composite Wind Turbine Blade", Embry-Riddle Aeronautical University

[6] "*Wind Turbine Airfoils*." Wind Turbine Airfoils. Web. 23 Nov. 2013.

[7] G. K. Batchelor. "An Introduction to Fluid Dynamics", Cambridge Univ.Press.Cambridge, England. (1967).

[8] Fluent, ANSYS FLUENT 12.0, Tutorial 9-11-12-23-28-29. Turbulence and Discrete Phase Modeling.

[9] P.J. Moriarty, A. C. Hansen; "AeroDyn Theory Manual" Technical Report National Renewable Energy Laboratory, January 2005; NREL/TP-500-36881.

[10] General Electric Company "*Technical Data of 1.5xle. pdf*", 2009. www.geosci.uchicage.edu/ moyer/GEOS24705/Readings/GEA14954C15-MW-broch.pdf

[11] Pramod Jain,"*Wind Energy Engineering*", McGraw-Hill Companies, 2011, ISBN: 978-0-07-171478-5.

[12] Brandon Burnett, "*COUPLED FLUID-STRUCTURE INTERACTION MODELING OF APARAFOIL*", Master of Science in Aerospace Engineering, Faculty of Embry-Riddle Aeronautical University, December 2016.

[13] M. M. Hand, D. Simms, L. Fingersh, D. Jager, J. Cotrell, S. Schreck, et al., Unsteady aerodynamics experiment phase VI: wind tunnel test configurations and available data campaigns: National Renewable Energy Laboratory Golden, Colorado, USA, 2001.

[14] http://www.arising.com.au/aviation/windturbines/wind-turbine.html; accessed on 01-06-2016.

[15] F. R. Menter, "Z*onal two equation k-turbulence models for aerodynamic flows*," AIAA paper,731 vol. 2906, p. 1993, 1993.

[16] W. Jones and B. Launder, "*The prediction of laminarization with a two-equation model of 733 turbulence*," International journal of heat and mass transfer, vol. 15, pp. 301-314, 1972.

[17] D. Wilcox and F. by Institutions, "*Formulation of the k-omega Turbulence Model Revisited*."

[18] https://en.wind-turbine-models.com/turbines/656-ge-general-electric-ge-1.5xle#